



Mechanism of dopant-vacancy association in -quartz GeO₂

H. Wang, A. Choneos, and U. Schwingenschlögl

Citation: *Journal of Applied Physics* **113**, 083716 (2013); doi: 10.1063/1.4793786

View online: <http://dx.doi.org/10.1063/1.4793786>

View Table of Contents: <http://scitation.aip.org/content/aip/journal/jap/113/8?ver=pdfcov>

Published by the [AIP Publishing](#)



Re-register for Table of Content Alerts

Create a profile.



Sign up today!



Mechanism of dopant-vacancy association in α -quartz GeO₂

H. Wang,¹ A. Chroneos,^{2,3} and U. Schwingenschlöggl^{1,a)}

¹PSE Division, KAUST, Thuwal 23955-6900, Saudi Arabia

²Department of Materials, Imperial College London, London SW7 2AZ, United Kingdom

³Materials Engineering, The Open University, Milton Keynes MK7 6AA, United Kingdom

(Received 29 December 2012; accepted 13 February 2013; published online 28 February 2013)

Improving the electron mobility of devices such as Ge metal oxide semiconductor field effect transistors requires good Ge/dielectric interfaces. GeO₂ thus is reconsidered as a passivation layer for Ge. However, O-vacancies need to be controlled as they have a deleterious impact on the properties. We employ electronic structure calculations to investigate the introduction of trivalent ions (Al, Y, and La) in α -quartz GeO₂. The binding energies of the dopant-vacancy pairs reveal that dopants can be used to control the O-vacancies and reduce the induced dangling bonds. It is proposed that the introduction of Al will limit the concentration of O-vacancies at low Fermi energy. © 2013 American Institute of Physics. [<http://dx.doi.org/10.1063/1.4793786>]

I. INTRODUCTION

Materials such as Ge are being actively considered as candidates for mainstream microelectronic applications.¹⁻⁹ Previous investigations have proposed that it is very important to form good Ge/dielectric interfaces (with reduced interface state density) to improve the electron mobility of Ge metal oxide semiconductor field effect transistors (Ge-MOSFETs).^{10,11} In the past, GeO₂ was introduced as passivation layer for Ge, however, without success due to its chemical and thermal instabilities. Over the past decade, research has focused on high-*k* dielectrics, resulting in the fabrication of the first Ge *p*- and *n*-MOSFETs. The introduction of high-*k* dielectrics such as HfO₂ and ZrO₂ can lead to a lowering of the equivalent oxide thickness and sharpening of the Ge/dielectric interface.¹²⁻¹⁴ However, the performance is compromised by the inability to achieve a low equivalent oxide thickness and good interface quality simultaneously. Presently, there is a trend to readdress the incorporation of GeO₂ as a possible passivation layer (Ge/GeO₂/high-*k* dielectric stack). However, this requires the improvement of the GeO₂ as well as its interface with Ge.¹⁵⁻¹⁷ There are two main issues that need to be rectified as they impact the quality of the GeO₂ passivation layer. First, volatile GeO is formed at temperatures typical of transistor processing.¹⁸ Previous studies suggest that mobile O vacancies are key to the formation of volatile GeO species.^{19,20} Second, at Ge/GeO₂ interfaces dangling bonds form, which have a deleterious impact on the electron mobility of devices.²¹ Both these issues can be resolved if the vacancies can be controlled.

Interestingly, Lee *et al.*²² have proposed a defect engineering strategy called “valency passivation” in which trivalent ions are introduced in GeO₂ near the interface with Ge. It is found that the inclusion of Y is beneficial for *n*-MOSFETs. Every O vacancy will introduce two dangling bonds, while a trivalent ion at a substitutional Ge position will reduce this number by one. In particular, the authors have observed an increase of the electron mobility at low

temperatures, resulting from a significant reduction of the density of interface states. For crystalline α -quartz GeO₂, previous work has only considered Y as a way to control O vacancies.²³

Control of O vacancies will positively impact the stability (by the reduction of the volatile GeO) and electrical properties (by the reduction of the dangling bonds) of GeO₂, paving the way to good MOS devices based on Ge. In the present study, we use density functional theory to investigate the impact of the trivalent ions Al, Y, and La in O deficient α -quartz GeO₂, aiming at understanding the advantages and drawbacks of the different dopants.

II. METHODOLOGY

Our calculations are based on density functional theory and the generalized gradient approximation of Perdew and Wang,²⁴ as implemented in the Vienna *ab-initio* simulation package.²⁵ An energy cutoff of 400 eV and projector-augmented waves are employed.²⁶ For testing the convergence of the supercell size, the O vacancy formation energy is compared for different supercell sizes until the difference is deemed to be insignificant. This is the case for a supercell of 72 atoms. A 4 × 4 × 4 *k*-point mesh is generated according to the Monkhorst-Pack scheme.²⁷ This mesh is well converged as the total energy changes by less than 1 meV/atom as compared to 6 × 6 × 6 and 8 × 8 × 8 *k*-point meshes. The experimental structures²⁸ are fully optimized until the remaining atomic forces are less than 0.01 eV/Å.

The employed supercell of α -quartz GeO₂, which crystallizes in a hexagonal structure, is shown in Fig. 1. Ge is located in the center of an O tetrahedron, where each O atom is shared by two tetrahedra. In the above supercell, one O atom is removed to form an O vacancy and one Ge atom is replaced by a dopant atom. For these configurations, the partial densities of states (DOSs) of atoms surrounding the vacancy are investigated.

Defect formation is effectively an exchange between the host material and an atomic (and/or electronic) reservoir. The formation energy of the defect is given by²⁹

^{a)}E-mail: Udo.Schwingenschlöggl@KAUST.edu.sa. Tel.: +966(0)544700080.

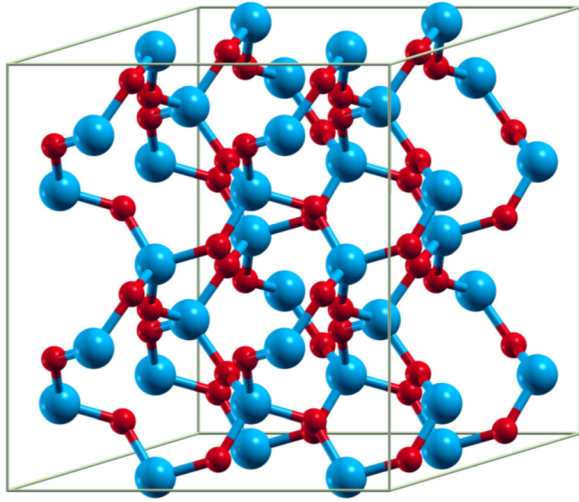


FIG. 1. Supercell structure of α -quartz GeO_2 . Large and small spheres represent Ge and O, respectively.

$$\Delta H_{G,q}(\mu_e, \mu) = E_{D,q} - E_H + n \cdot \mu + q \cdot \mu_e, \quad (1)$$

where $E_{D,q}$ is the total energy of the defective cell with charge q , E_H is the total energy of the perfect cell, n is the number of atoms added (or removed), $\mu = 1/2 \cdot E(\text{O}_2)$ is the chemical potential, and μ_e is the Fermi energy. The latter is measured from the top of the valence band.

To investigate the energetics of dopant-vacancy pairs and to be able to facilitate comparison between the different dopants, we calculate binding energies. The binding energy for substitution of an atom D at a Ge site in the presence of an O vacancy (V) in GeO_2 is given by

$$\begin{aligned} E_b(DVGe_{N-1}O_{2N-1}) = & E(DVGe_{N-1}O_{2N-1}) \\ & - E(DGe_{N-1}O_{2N}) - E(VGe_{N-1}O_{2N-1}) \\ & + E(Ge_{N-1}O_{2N}), \end{aligned} \quad (2)$$

where $E(DVGe_{N-1}O_{2N-1})$ is the energy of a supercell with $3N$ atoms (here: $3N=72$) containing one D and one O vacancy. Moreover, $E(DGe_{N-1}O_{2N})$ is the energy of a supercell containing one D , $E(VGe_{N-1}O_{2N-1})$ is the energy of a supercell containing one O vacancy, and $E(Ge_{N-1}O_{2N})$ is the energy of a supercell of pristine GeO_2 . With this definition, a negative binding energy corresponds to a DV pair that is stable with respect to its constituent point defect components.

III. RESULTS AND DISCUSSION

We find binding energies of -1.63 eV for LaV, -1.42 eV for YV, and -0.51 eV for AlV pairs. Therefore, all the DV pairs considered can form. For the LaV pair, the La-O bond distances (2.16 Å, 2.21 Å, and 2.23 Å) are smaller as compared to the case of La substitution (2.23 Å, 2.23 Å, 2.24 Å, and 2.24 Å). This is also the case for the YV pair (Y-O bond distances 2.07 Å, 2.09 Å, and 2.12 Å) and for the AlV pair (Al-O bond distances 1.69 Å, 1.71 Å, and 1.71 Å) as compared to Y substitution (2.12 Å, 2.12 Å, 2.15 Å, and 2.15 Å) and Al substitution (1.76 Å, 1.76 Å, 1.77 Å, and 1.77 Å), respectively.

All the partial DOSs investigated in this paper refer to the charge neutral system. The partial DOS of pristine GeO_2 (not shown) reveals two groups of bands in the energy range from -5 eV to the valence band maximum, separated by an energy gap. Both are dominated by O 2p states. There is a significant hybridization between the Ge 4p and O 2p states, where the Ge 4p states are more prominent in the lower energy range. The formation of an O vacancy results in two additional impurity states, which are located at -3.6 eV and -0.1 eV. Undoped GeO_2 without and with O vacancy is insulating with a band gap of 3.3 eV and 3.2 eV, respectively.

Spin polarized calculations are performed for Al, Y, and La doped GeO_2 without O vacancy, because doping of

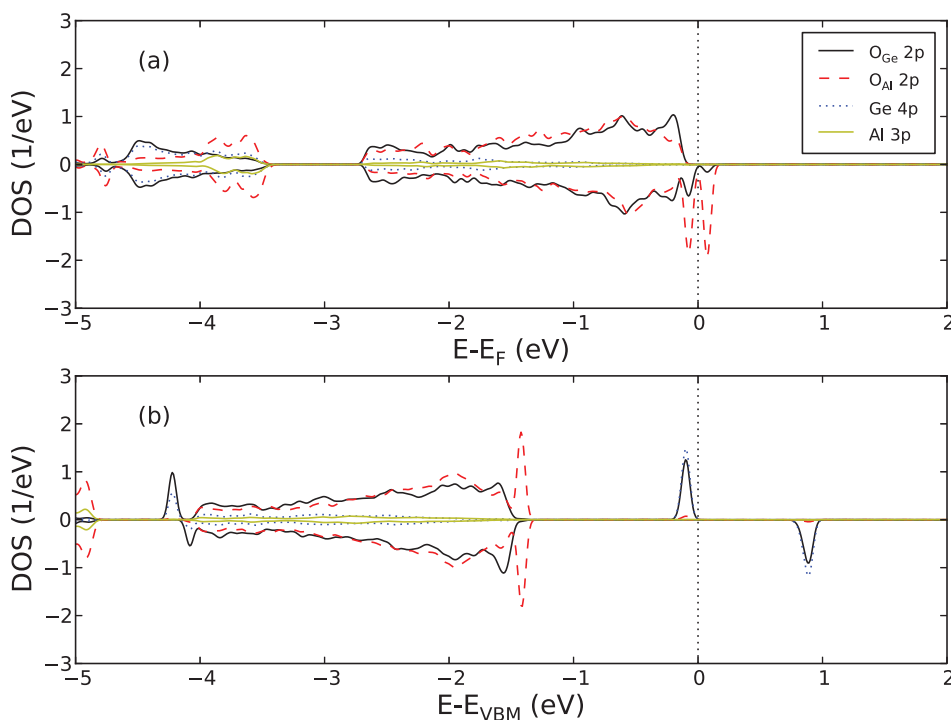


FIG. 2. Partial O 2p, Al 3p, and Ge 4p DOSs averaged over the atoms surrounding the O vacancy site in Al doped GeO_2 (a) without and (b) with O vacancy.

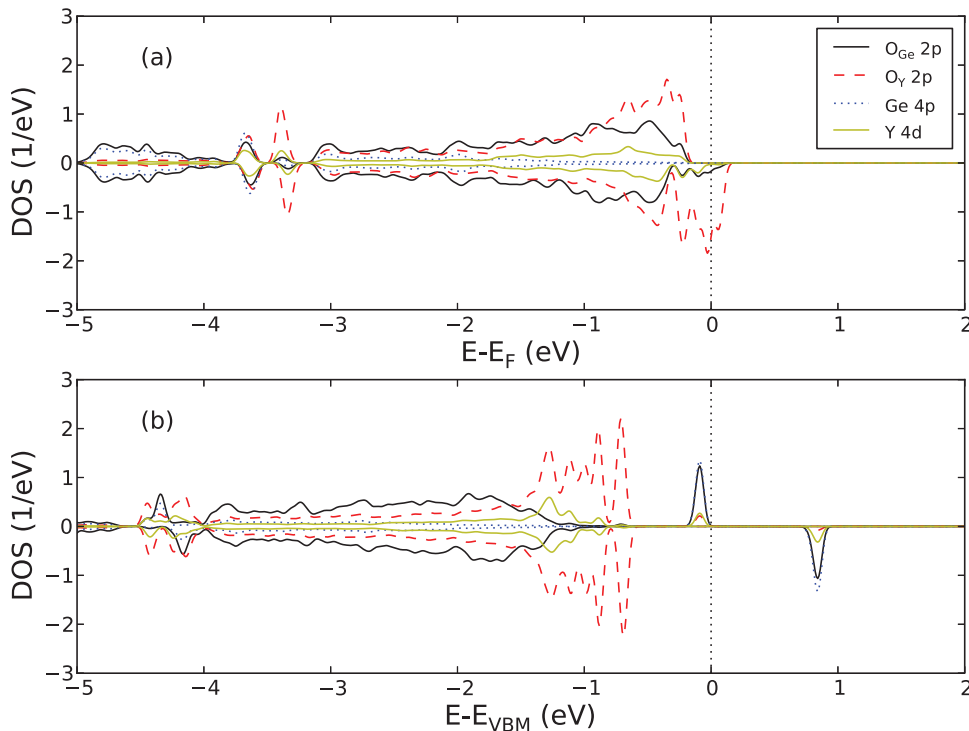


FIG. 3. Partial O 2p, Y 4d, and Ge 4p DOSs averaged over the atoms surrounding the O vacancy site in Y doped GeO_2 (a) without and (b) with O vacancy.²³

trivalent ions may result in local magnetic moments around the dopant, see the partial DOSs shown in Figs. 2(a)–4(a). The bottom panels of these figures correspond to AlV, YV, and LaV pairs. The bands below the occupied impurity state hardly show any spin splitting. The figures represent the average of the partial DOSs of the nearest neighbour atoms of the O vacancy. O_{Ge} denotes the O atoms that bond to Ge and $\text{O}_{\text{Al/Y/La}}$ those connecting with dopants. The hole doping causes metallicity as is clearly indicated by the partial DOSs in Figs. 2(a)–4(a).

In Fig. 2(b), a strongly hybridized Ge/O impurity state due to one electron freed by the introduction of the O vacancy appears just below 0 eV. Another impurity state is located around 0.9 eV. The integration of the total DOS demonstrates that each impurity state corresponds to exactly one electron. Spatially, the impurity state is located mainly on Ge and O_{Ge} next to the O vacancy. However, there are also contributions to the impurity peak in the DOS from Al, O_{Al} , and atoms further away. In Fig. 2(b), the remarkable O_{Al} peak forming at the top of the O 2p bands at about -1.5 eV

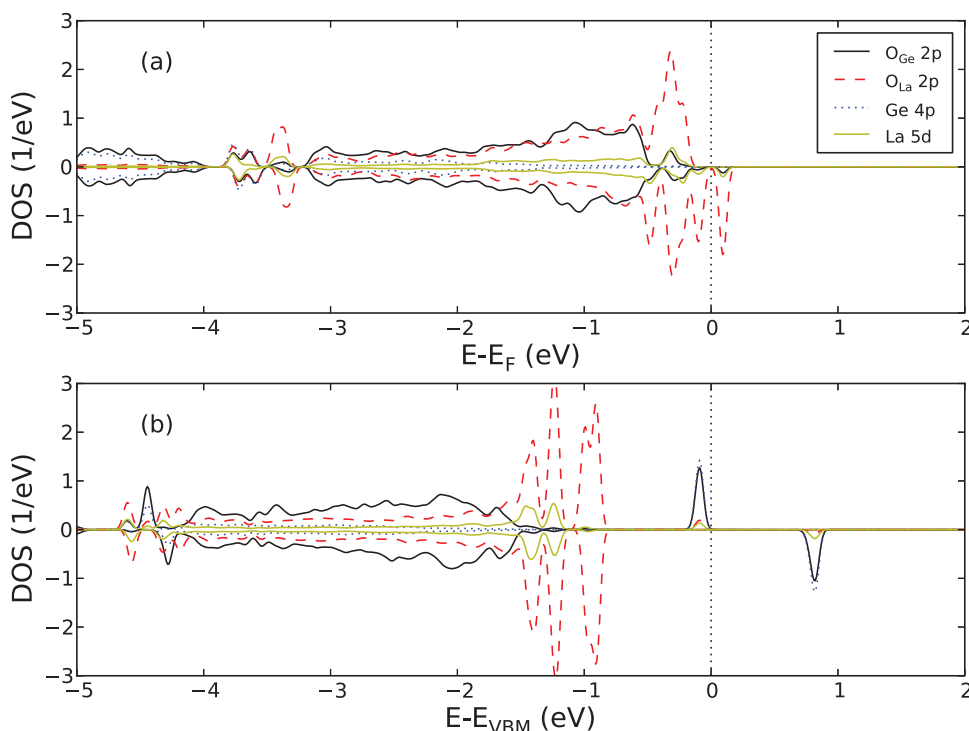


FIG. 4. Partial O 2p, La 5d, and Ge 4p DOSs averaged over the atoms surrounding the O vacancy site in La doped GeO_2 (a) without and (b) with O vacancy.

represents the O states that do not hybridize with other states.

For YV and LaV pairs, Figs. 3(b) and 4(b) also exhibit the occupied and unoccupied impurity states. The energy gap between them is almost 0.7 eV in both cases. The remarkable O_Y 2p and O_{La} 2p peaks at about -0.8 eV are again due to non-bonding O 2p orbitals. Doped GeO_2 without O vacancy, see Figs. 3(a) and 4(a), shows a group of localized states around -3.5 eV. Nevertheless, the dopants let the gap at lower energy vanish and enlarge the one below the impurity state. If both doping and O vacancies are present, these low energy features merge and the small energy gaps around them vanish. On the other hand, the energy gap which separates the impurity states from the localized O 2p states (around -0.8 eV) is significantly enlarged.

Comparing Figs. 3(a) and 4(a) to Fig. 2(a), we find that Y and La doped GeO_2 have more states near the Fermi level than in the case of Al doping. The reason is that the d orbitals of Y and La are more localized and directed than the Al p orbitals so that they overlap less with the O 2p orbitals. This means that Y-O and La-O bonds are less stable than Al-O bonds, which is consistent with the observation that the Y-O and La-O bonds are longer than the Al-O bonds. Thus, an O vacancy in Y and La doped GeO_2 is expected to be more favourable to form than in Al doped GeO_2 .

Fig. 5 summarizes the formation energies of O vacancies for a range of charge states, as a function of the Fermi energy (refer to Eq. (1)). It addresses both undoped and doped α -quartz GeO_2 . The +2 charged O vacancy formation energies of Y- GeO_2 and La- GeO_2 are more negative than that of GeO_2 , because the trivalent ions favor to lose one bond with O as compared to Ge. Ionization energies for O vacancies in undoped and doped GeO_2 are given in Table I. For undoped GeO_2 only the +2 and 0 charge states play a

TABLE I. Ionization energies (in eV) for O vacancies in pristine and doped GeO_2 .

	Pristine	Al	Y	La
$\varepsilon(++/0)$	2.47	1.61	2.66	2.47
$\varepsilon(++/+)$	3.87	0.23	1.35	1.13
$\varepsilon(+/-)$	4.59	2.31	3.25	3.17

role, the former at low Fermi energy and the latter at high Fermi energy, see Table I. The introduction of dopants lowers the upper end of the Fermi energy range, where the +2 charge state is favourable to 1.35 eV for Y, 1.13 eV for La, and to only 0.23 eV for Al. Even the -1 charge state can become favourable for very high values of the Fermi energy. It is observed that the plots for Y- GeO_2 and La- GeO_2 in Fig. 5 are very similar, while the differences for Al doped GeO_2 are more pronounced. In particular, in Al doped GeO_2 , the +2 charge state is only favourable close to zero Fermi energy and its formation energy is less negative than for Y and La doped GeO_2 for the reasons discussed above. For small Fermi energy, both undoped and doped α -quartz GeO_2 will be O deficient as O vacancies have negative formation energies. This is consistent with the previous studies, which have verified that O vacancies are the dominant intrinsic point defects in GeO_2 .^{30–32} We propose that a defect engineering strategy to limit O vacancies can be based on doping with Al, because the O vacancies are less favourable to form in Al doped GeO_2 than in the other two cases.

Al, therefore, is good to avoid O vacancies. However, there is a second issue to be considered. LaV and YV pairs have larger binding energies than AlV. This indicates that a dopant-vacancy pair is easier to form for La and Y than for Al doping. For this reason, La and Y are better suitable for

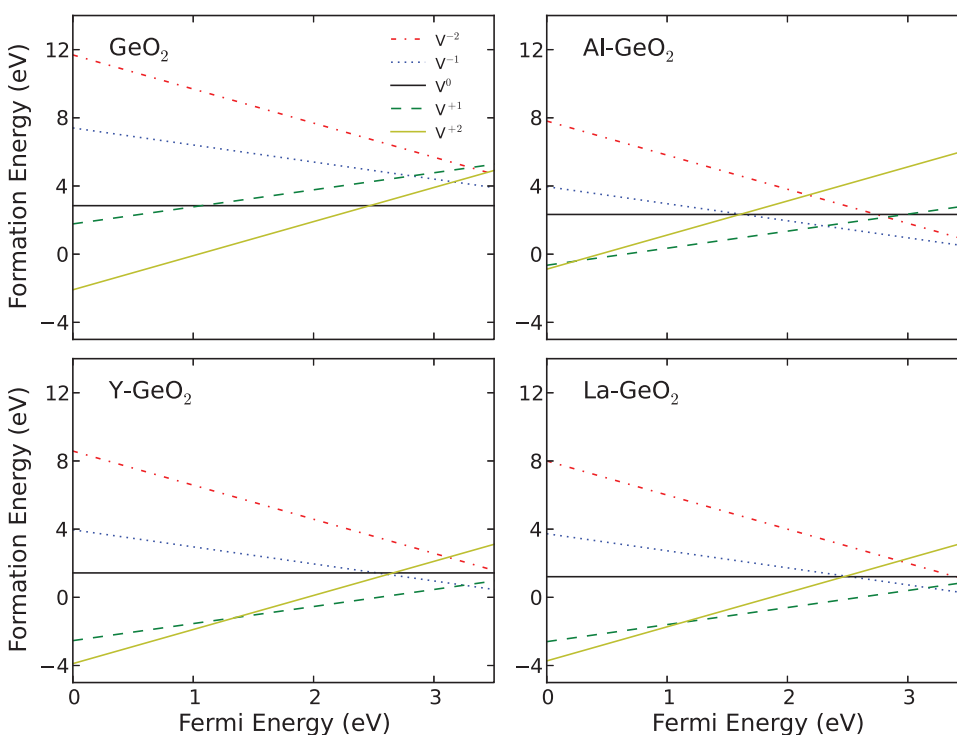


FIG. 5. Formation energies of an O vacancy as a function of the Fermi energy for pristine GeO_2 , Al doped GeO_2 , Y doped GeO_2 ,²³ and La doped GeO_2 .

controlling the diffusion of O vacancies, which achieves the desorption of volatile GeO in the Ge/GeO₂ interface.^{19,20} Experimentally, Y doping has proven to be a good strategy to improve the properties of Ge/GeO₂ interfaces²² by dramatically reducing the interface states density. La doping is predicted to have a very similar effect. While Al doping avoids the formation of O vacancies efficiently, Y and La doping are advantageous for trapping O vacancies. Therefore, all these dopants have potential to improve the properties of the device.

IV. CONCLUSIONS

In conclusion, we have used electronic structure calculations to investigate the association of trivalent dopants in α -quartz GeO₂. The doping of trivalent ions makes α -quartz GeO₂ metallic and results in localized magnetic moments. O vacancies cause occupied impurity states to appear below the Fermi level and unoccupied impurity states in the band gap. Al doped GeO₂ exhibits more stable bonds with O than the other two dopants so that its O vacancy formation energies are less negative. It is calculated that all three dopants considered form bound pairs with O vacancies, where bound pairs with Y and La are more stable. Consequently, it is expected that the introduction of Y and La will also limit the mobility of O vacancies and reduce the dangling bonds in α -quartz GeO₂, therefore, improving the quality of the Ge/GeO₂ interface. In addition, the introduction of Al is found to limit the O vacancy concentration at low Fermi energy.

¹A. Ritenour, S. Yu, M. L. Lee, N. Lu, W. Bai, A. Pitera, E. A. Fitzgerald, D. L. Kwong, and D. Antoniadis, Tech. Dig. - Int. Electron Devices Meet. **2003**, 03-433.

²G. Impellizzeri, S. Boninelli, F. Priolo, E. Napolitani, C. Spinella, A. Chroneos, and H. Bracht, *J. Appl. Phys.* **109**, 113527 (2011).

³C. O. Chui, L. Kulig, J. Moran, W. Tsai, and K. C. Saraswat, *Appl. Phys. Lett.* **87**, 091909 (2005).

⁴E. Simoen and J. Vanhellemont, *J. Appl. Phys.* **106**, 103516 (2009).

⁵S. Schneider and H. Bracht, *Appl. Phys. Lett.* **98**, 014101 (2011).

⁶E. Scalise, M. Houssa, G. Pourtois, V. V. Afanas'ev, and A. Stesmans, *Appl. Phys. Lett.* **98**, 202110 (2011).

⁷H. Tahini, A. Chroneos, R. W. Grimes, U. Schwingenschlögl, and H. Bracht, *Appl. Phys. Lett.* **99**, 072112 (2011).

⁸H. Tahini, A. Chroneos, R. W. Grimes, and U. Schwingenschlögl, *Appl. Phys. Lett.* **99**, 162103 (2011).

⁹W. S. Jung, J. H. Park, A. Nainani, D. Nam, and K. C. Saraswat, *Appl. Phys. Lett.* **101**, 072104 (2012).

¹⁰C. H. Lee, T. Nishimura, N. Saido, K. Nagashio, K. Kita, and A. Toriumi, Tech. Dig. - Int. Electron Devices Meet. **2009**, 09-457.

¹¹T. Nishimura, C. H. Lee, S. K. Wang, T. Tabata, K. Kita, K. Nagashio, and A. Toriumi, Dig. Tech. Pap. - Symp. VLSI Technol. **2010**, 209.

¹²K. Kita, K. Kyuno, and A. Toriumi, *Appl. Phys. Lett.* **85**, 52 (2004).

¹³A. Dimoulas, G. Mavrou, G. Vellianitis, E. Evangelou, N. Boukos, M. Houssa, and M. Caymax, *Appl. Phys. Lett.* **86**, 032908 (2005).

¹⁴A. Ritenour, A. Khakifirooz, D. A. Antoniadis, R. Z. Lei, W. Tsai, A. Dimoulas, G. Mavrou, and Y. Panayiotatos, *Appl. Phys. Lett.* **88**, 132107 (2006).

¹⁵A. Molle, M. N. K. Bhuiyan, G. Talarida, and M. Fanciulli, *Appl. Phys. Lett.* **89**, 083504 (2006).

¹⁶A. Delabie, F. Bellenger, M. Houssa, T. Conard, S. Van Elshocht, M. Caymax, M. Heyns, and M. Meuris, *Appl. Phys. Lett.* **91**, 082904 (2007).

¹⁷H. Matsubara, T. Sasada, M. Takenaka, and S. Takagi, *Appl. Phys. Lett.* **93**, 032104 (2008).

¹⁸K. Prabhakaran, F. Maeda, Y. Watanabe, and T. Ogino, *Appl. Phys. Lett.* **76**, 2244 (2000).

¹⁹S. K. Wang, K. Kita, C. H. Lee, T. Tabata, T. Nishimura, K. Nagashio, and A. Toriumi, *J. Appl. Phys.* **108**, 054104 (2010).

²⁰S. K. Wang, K. Kita, T. Nishimura, K. Nagashio, and A. Toriumi, *Jpn. J. Appl. Phys., Part 1* **50**, 04DA01 (2011).

²¹C. H. Lee, T. Tabata, T. Nishimura, K. Nagashio, K. Kita, and A. Toriumi, *Appl. Phys. Express* **2**, 071404 (2009).

²²C. H. Lee, T. Nishimura, T. Tabata, S. K. Wang, K. Nagashio, K. Kita, and A. Toriumi, Tech. Dig. - Int. Electron Devices Meet. **2010**, 10-416.

²³H. Wang, A. Chroneos, A. Dimoulas, and U. Schwingenschlögl, *Phys. Chem. Chem. Phys.* **14**, 14630 (2012).

²⁴J. P. Perdew and Y. Wang, *Phys. Rev. B* **45**, 13244 (1992).

²⁵G. Kresse and J. Joubert, *Phys. Rev. B* **59**, 1758 (1999).

²⁶P. E. Blöchl, *Phys. Rev. B* **50**, 17953 (1994).

²⁷H. J. Monkhorst and J. D. Pack, *Phys. Rev. B* **13**, 5188 (1976).

²⁸G. S. Smith and P. B. Isaacs, *Acta Crystallogr.* **17**, 842-846 (1964).

²⁹S. Lany and A. Zunger, *Phys. Rev. B* **78**, 235104 (2008).

³⁰M. Yang, R. Q. Wu, Q. Chen, W. S. Deng, Y. P. Feng, J. W. Chai, J. S. Pan, and S. J. Wang, *Appl. Phys. Lett.* **94**, 142903 (2009).

³¹P. Broqvist, J. F. Binder, and A. Pasquarello, *Appl. Phys. Lett.* **97**, 202908 (2010).

³²K. Kita, T. Takahashi, H. Nomura, S. Suzuki, T. Nishimura, and A. Toriumi, *Appl. Surf. Sci.* **254**, 6100 (2008).